Optical absorption behaviour of platinum core–silica shell nanoparticle layer and its influence on the reflection spectra of a multi-layer coating system in the visible spectrum range

2004 J. Phys.: Condens. Matter 16 3199

(http://iopscience.iop.org/0953-8984/16/18/020)

INSTITUTE OF PHYSICS PUBLISHING JOURNAL OF PHYSICS: CONDENSED MATTER

J. Phys.: Condens. Matter **16** (2004) 3199–3206 PII: S0953-8984(04)76123-8

Optical absorption behaviour of platinum core–silica shell nanoparticle layer and its influence on the reflection spectra of a multi-layer coating system in the visible spectrum range

Sang Woo Kim[1], Dong-Sik Bae[2], Hyunho Shin[3,4] and Kug-Sun Hong[3]

[1] Nanomaterials Research Centre, Korea Institute of Science and Technology, Seoul 136-791, Korea
[2] Department of Ceramics Engineering, Changwon National University, Kyongnam 641-773, Korea
[3] School of Materials Science and Engineering, Seoul National University, Seoul 151-744, Korea

E-mail: hshin@snu.ac.kr

Received 10 February 2004
Published 23 April 2004
Online at stacks.iop.org/JPhysCM/16/3199
DOI: 10.1088/0953-8984/16/18/020

Abstract

Platinum core–silica shell nanoparticles (Pt@SiO_2) have been applied to the outermost layer of a three-layer film structure to yield a Pt@SiO_2/SiO_2/ITO (indium tin oxide) coating on a glass substrate. Optical properties of the three-layer film have been investigated in the visible spectrum regime. The absorption of visible light by the Pt core–SiO_2 shell layer was higher in low- and high-wavelength regimes while it was minimal at a mid-visible light range, about 550 nm. This characteristic absorption of the core–shell layer resulted in a broad-band anti-reflectance behaviour of the multi-layer coating system in the entire visible light regime. Transmittance of the three-layer coating–glass system was in the range between 80% and 85% and thus the application of the platinum core–silica shell nanoparticle layer with such absorption characteristics is shown to provide flexibility of ways to achieve a broad-band anti-reflectance and transmittance of a multi-layer coating system.

1. Introduction

Nanoscale metal particles in the size range 1–10 nm, as compared to their bulk counterpart, exhibit unique properties different from the bulk state such as unusually high optical absorption [1, 2], size quantization [3], non-linear optical behaviour [4], surface-enhanced Raman scattering [5], and unusual fluorescence [6]. Characteristic optical absorption is caused

[4] Author to whom any correspondence should be addressed.

by the plasmon modes of conduction electrons in metal particles which are coupled with the transverse electromagnetic field through the particle–medium interface [7, 8]. Consequently, the absorption peak position is dependent on the type of environment medium [7, 8], e.g., it yields an absorption in the visible range when the particles (Au, Ag, Cu, etc) are embedded in solids [2, 9–14]. The peak position is also dependent on particle size [1, 2, 15–17], and particle loading fraction in the medium [11, 18]. Thus, the theoretical prediction of the peak position has been the subject of high interest [7, 8, 18]. However, the characteristic optical absorption peaks of nanosized metals broaden significantly [9, 15, 19–21] when the particle is small compared to the mean free path of the conduction electrons due to the scattering of the electrons from the particle surfaces [19]. The broadening of the resonance peak is also strongly dependent on the particle–medium chemical interface characteristics [20]. It is also often reported that the characteristic absorption peak even disappears and thus only a broad-band absorption takes place [10, 22–25]. In the light of the work of Mu *et al* [24] and Schroeder *et al* [26], the peak disappears when the metals fail to form a cluster or colloid, i.e., when they are in atomic state. Even when metals form a cluster, the absorption peak can disappear depending on the particle–medium chemical interface state [24].

The unusually high optical absorption of nanosized metal particles in the visible spectrum, together with the broad-band absorption characteristics (absence of the characteristic absorption peak), has a potential to yield a broad-band anti-reflectance, since the reflectance is reduced by an increase in absorptance [27]. Morimoto *et al* [25] reported a result consistent with this view. In their work, a notable broad-band anti-reflection was observed when they applied a coating with nanosized metal (Ag) particles on a glass substrate, which result may be associated with the role of the ultra-fine metal particles having broad-band absorption characteristics. In a recent work [22], a well separated platinum nanoparticle in a silica medium also demonstrated the high-broad-band-absorption characteristics, unlike bulk platinum [28].

From the viewpoint of the broad-band optical absorption, especially in the visible spectrum range, the platinum nanoparticle has a benefit in that the characteristic absorption peak is in the ultraviolet (210–300 nm) range [29–31] unlike other metal nanoparticles (Au, Ag, Cu, etc) which are in the visible range. The absorption by platinum nanoparticles decays smoothly in the direction of longer wavelengths, i.e., in the visible spectrum range. Thus, even when the characteristic peak does not disappear in the ultraviolet range, one can safely exploit the high absorption of platinum nanoparticles with the broad-band absorption characteristics in the visible spectrum range.

In the present study, a silica film loaded with platinum nanoparticles ($Pt@SiO_2$) was applied as a coating to a visible-range-transparent soda-lime glass substrate. The glass substrate was pre-coated with silica and indium tin oxide (ITO) films so that the multi-layer system was $Pt@SiO_2/SiO_2$/ITO/glass substrate. In this work, the separation of platinum nanoparticles in the outermost layer was achieved by pre-coating the individual platinum particle core with a silica shell ($Pt@SiO_2$). Then, the capability of a broad-band absorption of the $Pt@SiO_2$ nanoparticle film and its influence on the overall reflectance of the multi-layered system were investigated in the visible spectrum range.

2. Experimental procedure

The use of three-layer coating systems in order to provide electrical conductivity as well as broad-band anti-reflection for many applications is well documented [32, 33] including the use of ITO and SiO_2 as the first and the second layer, respectively. In the present study, a thin film dispersed with platinum core–silica shell particles was applied to the third (outermost) layer. For each coating layer, three types of corresponding solution were prepared as follows. For

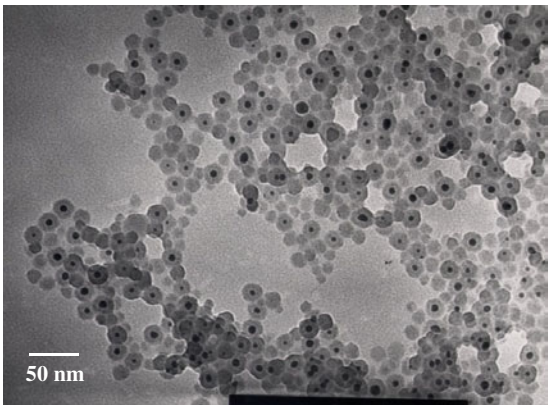

Figure 1. Transmission electron micrograph of the platinum core–silica shell ($Pt@SiO_2$) nanoparticles.

the first ITO layer coating, a 7 at.% Sn-doped indium oxide powder (average particle size of 60 nm) was mixed in ethanol medium to form a 5 wt% ITO particle-dispersed solution. After subsequent ultrasonic treatment and ball milling of the solution, ethanol was further added to prepare a 1.8 wt% ITO particle-dispersed solution. For the second layer (silica) coating, a mixed solution of TEOS (tetraethylorthosilicate, Wako, Japan), ethanol, and hydrochloric acid was stirred at 40 °C for 2 h, followed by hydrolysis and condensation to prepare a pure silica sol. Finally, for the third $Pt@SiO_2$ layer coating, the platinum core–silica shell particles were prepared by reverse micelles followed by *in situ* hydrolysis and condensation in the microemulsions. The detailed synthesis procedure is described elsewhere [34, 35]. The obtained powders were re-dispersed in alcohol solutions to prepare a silica-coated platinum particle ($Pt@SiO_2$) solution.

The films were prepared by the spin coating method on the soda-lime glass substrate ($100 \times 100 \times 0.5$ mm^3) which was cleaned with a CeO_2 solution and heated in an oven at 50 °C. The ITO layer and the silica layer were coated on the glass substrate, sequentially. Coated glasses were dried in air for 1 h and heat-treated up to 180 °C with a heating rate of 4 °C min^{-1}. The temperature was kept for 30 min and then lowered to room temperature. The over-coated silica was amorphous and microporous. Finally, the outermost layer was coated by spin coating using the $Pt@SiO_2$ solution on the silica/ITO/glass substrate system. Only a single side of the glass substrate was multi-coated as above, followed by final heat-treatment at 180 °C for 30 min in air.

The total reflectance and the total transmittance of the multi-layer films were investigated using the UV visible–near-IR spectrometer (Perkin Elmer, Lamda-19, USA). Barium sulphate was used as a reference material for total reflectance measurement and the incident angle of the beam onto the sample was 90°. The morphologies of the platinum core–silica shell nanoparticles and the cross-sectional morphologies of the multi-layer films were characterized by transmittance electron microscopy (Phillips, JEM-200CX) and field emission scanning electron microscopy (Hitachi, S-4200, Japan), respectively.

3. Results

Figure 1 shows a transmission electron microscopy (TEM) image of the nanosized platinum–silica core–shell particles. The shape of the $Pt@SiO_2$ particles was spherical and the particle size was within the range from 10 to 20 nm. Figure 2 shows the cross-section microstructures

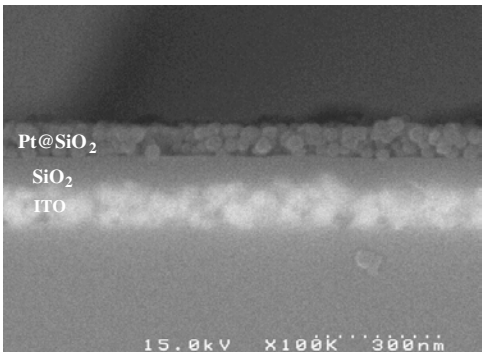

Figure 2. Field emission scanning electron micrograph of the cross-sectional view of the specimen subject to the optical property measurement.

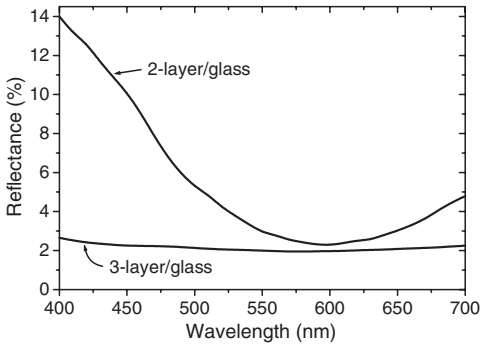

Figure 3. Reflectance spectra from SiO_2/ITO/glass (two-layer–glass) and Pt@SiO_2/SiO_2/ITO/glass (three-layer–glass) specimens.

of the three coating layers observed in field emission scanning electron microscopy (FE-SEM). The thicknesses of the three layers on the glass substrate were about 85/70/100 nm, respectively.

Figure 3 shows the reflectance spectra from the Pt@SiO_2/SiO_2/ITO three-layer film and the SiO_2/ITO two-layer film. The reflectance of the three-layer–glass system is less than 3% in the entire visible range, i.e., a broad-band anti-reflectance is achieved. However, the reflectance of the two-layer–glass specimen shows a minimum at about 600 nm and a rather high reflectance at other wavelengths.

The transmittance spectra of the Pt@SiO_2/SiO_2/ITO three-layer film and the SiO_2/ITO two-layer film are compared in figure 4. The three-layer–glass system shows diminished transmittance as compared to the two-layer–glass system throughout the entire visible range. However, the transmittance of the platinum-loaded three-layer–glass system is still fairly high, i.e., 80%–85%.

4. Discussion

4.1. Effective absorptance of Pt@SiO_2 layer

The significant reduction of the reflectance shown in figure 3 with the application of the platinum nanoparticle-embedded layer is indeed of interest. Such a phenomenon is associated with the fact that the optical behaviour of platinum nanoparticles is totally different from the bulk counterpart which has about 99.7% reflectance in the visible range [28]. In order to seek the role of the platinum nanoparticle-dispersed outermost layer on such a broad-band anti-reflectance of the three-layer–glass system, it is worthwhile to uncover the effective absorptance solely by the nanoparticle-embedded layer. Using the reflectance (figure 3) and transmittance (figure 4) results, effective absorption spectra of the specimens were constructed in figure 5, based on the relation

$$R = 1 - R - T \tag{1}$$

where R is the reflectance, A is the absorptance, and T is the transmittance. In fact, the absorptance of a multiplayer system obtained by this way contains the true absorption effect as well as the interference effect, unlike a thick monolithic bulk system which has the true absorptance effect only. Therefore, we used the term 'effective' absorption for the multiplayer system herein. As seen in figure 5, the effective absorptance of the three-layer–glass system is minimal at about 525 nm, while that of the two-layer–glass system increases gradually with

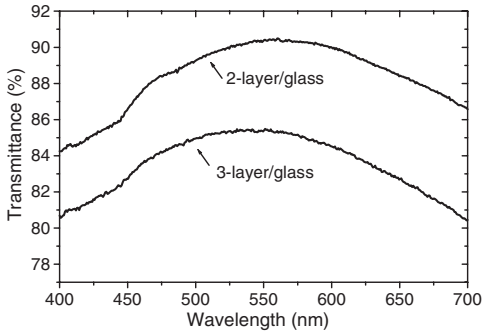

Figure 4. Transmittance spectra from SiO_2/ITO/glass (two-layer–glass) and Pt@SiO_2/SiO_2/ITO/glass (three-layer–glass) specimens.

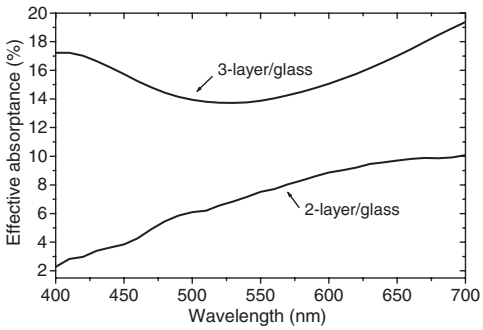

Figure 5. Absorptance spectra from SiO_2/ITO/glass (two-layer–glass) and Pt@SiO_2/SiO_2/ITO/glass (three-layer–glass) specimens.

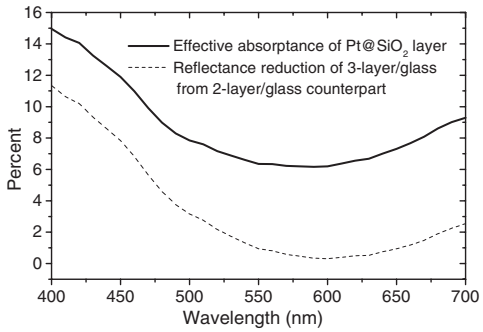

Figure 6. Comparison of the effective absorptance of the Pt@SiO_2 layer (solid curve) with the reflectance reduction from the two-layer–glass to the three-layer–glass (dashed curve).

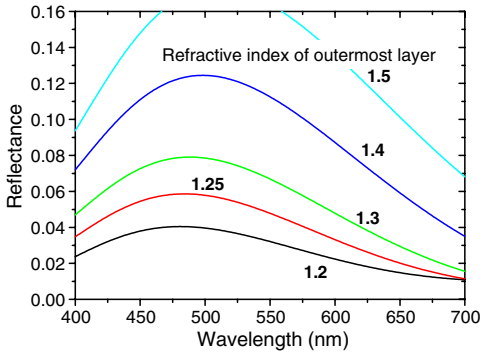

Figure 7. Reflectance simulation when an 85 nm thick non-absorbing layer with varying refractive index values is coated on the two-layer–glass system as the outermost layer.

(This figure is in colour only in the electronic version)

wavelength. The difference of the effective absorptance between the three-layer–glass system and the two-layer–glass system would solely result from the effective absorption behaviour of the Pt@SiO_2 outermost layer. Thus, the difference is illustrated in figure 6 as a function of wavelength to elucidate the effective absorptance by the Pt@SiO_2 layer (solid curve).

In figure 6, the effective absorption by the platinum core–silica shell layer (solid curve) is fairly high as compared with the absorptance of the bulk platinum (about 0.3% in the visible range [28]), primarily due to the high-absorption characteristics of the platinum nanoparticles [22]. The effective absorption spectrum does not show any characteristic absorption peak but a broad-band absorption behaviour [29–31].

4.2. Influence of Pt@SiO_2 layer absorption on anti-reflection of overall system

Having shown the effective absorption behaviour of the Pt@SiO_2 layer, it is now necessary to investigate how such behaviour is correlated with the apparent broad-band anti-reflection behaviour of the overall three-layer–glass system shown in figure 3. Included in figure 6 is

the difference between the reflectance of the three-layer–glass system and the two-layer–glass system (dashed curve), determined from figure 3. As apparent in figure 6, the trends in two curves are similar. When the effective absorption (solid curve) by the Pt nanoparticle layer is high, e.g., at wavelengths below about 550 nm, the diminution of the reflectance by the presence of the nanoparticle layer (dashed curve) is more apparent. This indicates that the effective absorption behaviour of the Pt@SiO_2 layer is closely related to the characteristic reflectance reduction in the three-layer–glass system as compared to the two-layer–glass (figure 3).

The influence of the effective absorption behaviour of the Pt@SiO_2 layer shown in figure 6 on the overall anti-reflection of the three-layer–glass system is qualitatively pursued as follows. The Pt@SiO_2 layer is deduced to lower the first-order reflectance from the three-layer–glass system. Consider the reflectivity of an infinitely thick medium [27]:

$$R_\infty = 1 + \frac{\beta}{s} - \left(\frac{\beta^2}{s^2} + 2\frac{\beta}{s}\right)^{1/2} \tag{2}$$

where the reflectivity R_∞ is the reflectance (fraction of incident light to specularly or diffusely reflected) of an infinitely thick specimen, β is the absorption coefficient, and s is the scattering coefficient. Note that there is only first-order reflection in an infinitely thick medium. Assuming that the introduction of nanosized metal particles to the medium does not affect the scattering coefficient as the size is much smaller than the wavelength of light, increase in coefficient of absorption by the metal particles is anticipated to yield the low first-order reflectance of the metal-loaded specimen.

The platinum-dispersed layer would diminish the higher-order reflectance as well in the three-layer–glass system. As far as such violet and red light regimes are concerned, an enhanced true absorption by the outermost layer would result in an increased blockage of light travelling through the Pt@SiO_2 layer: both the (reflected) light travelling toward the buried two-layer coating and the reflected light from the buried layers[5]. From the reduction of the first- and higher-order reflection by the Pt@SiO_2 layer as mentioned above, the high effective absorption of the platinum nanoparticle-loaded layer especially in violet and red light regimes is speculated to be responsible for the overall broad-band anti-reflection behaviour of the three-layer–glass system (figure 3).

4.3. Further discussion—methods solely relying on interference effect

Actually, the broad-band anti-reflection behaviour can also be obtained via proper design of *non-absorbing* homogeneous multi-layer films by solely relying on the interference effect: by an appropriate selection of optical parameters of each layer, i.e., refractive index and respective thickness [36]. In order to evaluate the required refractive index of the outermost layer if a non-absorbing film is applied for such layer, reflection of the three-layer–glass system is simulated based on the Fresnel equation [36] using varying refractive indices of the outermost layer, and the result is shown in figure 7. For the calculation, refractive indices of the porous ITO (100 nm thick) and porous SiO_2 (70 nm thick) layer are 1.71 and 1.30, respectively[6]. The simulated thickness of the outermost layer was 85 nm with refractive indices between 1.2 and 1.5. It turns out in figure 7 that the broad-band anti-reflection as seen in figure 3 can be achieved when the refractive index of the outermost layer is as low as 1.2. The role of the Pt@SiO_2 layer in

[5] The diminution of higher-order *reflection* due to the true absorption of the Pt nanoparticle layer implies that the effective absorption being discussed in this work mainly consists of the true absorption effect instead of the interference effect (destructive interaction between *reflected* beams of different orders).

[6] These values were obtained via the Lorentz–Lorentz relation [37] considering the porosity of each layer, i.e., 29%, and 19% respectively, which was determined from a separate experiment. The SiO_2 and ITO film were assumed as non-absorbing media for the calculation.

this work is indeed similar to the 85 nm thick non-absorbing layer having a very low refractive index of 1.2. Realizing such a low value of refractive index using a non-absorbing film material (by solely relying on the interference effect) is practically difficult. A feasible way to decrease refractive index involves the introduction of pores (refractive index, $n = 1.0$) to the sol–gel derived silica ($n = 1.458$). In the light of the Lorentz–Lorentz relation, embedded pores (refractive index, $n = 1.003$) in solid medium reduces the refractive index practically linearly by the relation [37],

$$\left(n_c^2 - 1\right)\left(n_c^2 + 2\right) = (1 - P)\left(n_s^2 - 1\right)\left(n_s^2 + 2\right) \tag{3}$$

where n is the refractive index, P is the porosity, and subscripts s and c denote solid skeleton and pore/solid skeleton composite system, respectively. In order to achieve a refractive index of 1.2, a porosity of about 47% in silica is required, which certainly causes a significant loss in mechanical stability [38]. Thus, the practical demonstration of the anti-reflectance in the entire visible range is not an easy task, if one solely relies on non-absorbing films. In general, meeting the designed optical parameters at each layer via appropriate material processing requires much more endeavour than the design effort, which, in turn, limits the design flexibility.

Another notable approach for achieving the broad-band anti-reflection behaviour based on the interference effect is the employment of the surface gratings in the sub-wavelength scale, i.e., a few hundred nanometres, at the outermost layer in the multi-layer film structure [39]. Such a surface relief structure can be made by surface etching, micromachining, or introduction of porous coatings via the sol–gel route to yield surface modulation. However, the typical three layer anti-reflective films either produced via the vacuum technique [32] or sol–gel coatings [33] have shown higher reflectance at wavelengths higher or lower than around 600 nm, due to the processing-related design limitations.

The low reflectance in the entire visible range is a characteristic feature of the current three-layer coating, which utilizes the partially absorbing Pt@SiO_2 outermost layer. It is noted that, although the silica-coated platinum nanoparticle layer has some absorbing characteristics, the total transmittance of the three-layer–glass system is fairly high, i.e., 80%–85% (figure 4). Thus, the demonstration of the broad-band anti-reflection via the utilization of the partially absorbing metal-dispersed layer in the current work provides flexibility of ways to practically achieve the multi-layer coating system which yields the broad-band anti-reflection as well as transparency characteristics.

5. Conclusions

Platinum core–silica shell nanoparticles (Pt@SiO_2) have been prepared via a reverse micelle method and applied as the outermost layer of a three-layer film structure to yield a Pt@SiO_2/SiO_2/indium tin oxide coating on glass. The Pt@SiO_2 layer showed characteristic optical absorption behaviour: the absorption was higher in violet (about 15%) and red light (about 9.2%) regimes while it was minimal (about 6.5%) at a mid-visible light range, about 550 nm. Such an absorption feature was directly related to a more efficient reduction of reflectance in violet and red light regimes, resulting in a broad-band anti-reflectance in the entire visible light regime. Since the transmittance of the three-layer coating–glass system was in the range between 80% and 85%, the application of the silica-coated platinum core–shell nanoparticle layer with such optical absorption characteristics is shown to provide a flexibility of ways to achieve a broad-band anti-reflectance and transmittance in the transparent multi-layer coating system.

References

[1] Ko M-J 1998 *Adv. Mater. Opt. Electron.* **8** 173
[2] Arnold G W and Borders J A 1977 *J. Appl. Phys.* **48** 1488
[3] Brus L E 1984 *J. Chem. Phys.* **80** 4403
[4] Jain R K and Lind R C 1983 *J. Opt. Soc. Am.* **73** 647
[5] Chen M C, Tsai S D, Chen M R, Ou S Y, Li W H and Lee K C 1996 *Phys. Rev.* B **51** 4507
[6] Misawa K, Yao H, Hayashi T and Kobayashi T 1991 *Chem. Phys. Lett.* **183** 113
[7] Nolte D D 1994 *J. Appl. Phys.* **76** 3740
[8] Persson B N J 1993 *Surf. Sci.* **281** 153
[9] Tanahashi I, Manabe Y and Tohda T 1996 *J. Appl. Phys.* **79** 1244
[10] Wang B and Zhang L 1998 *Appl. Surf. Sci.* **133** 152
[11] Tang L, Du P, Han G, Weng W, Zhao Z and Shen G 2003 *Surf. Sci. Technol.* **167** 177
[12] Ando M, Kobayashi T and Haruta M 1997 *Catal. Today* **36** 135
[13] Ray A K, Exley J, Ghassemlooy Z, Crowther D, Ahmet M T and Silver J 2001 *Vacuum* **61** 19
[14] Duffy J A 1977 *J. Am. Ceram. Soc.* **60** 440
[15] Ganière J-D, Rechsteiner R and Smithard M-A 1975 *Solid State Commun.* **16** 113
[16] Preston C K and Moskovits M 1988 *J. Phys. Chem.* **92** 2957
[17] Kreibig U 1985 *Surf. Sci.* **156** 678
[18] Doremus R 1998 *Thin Solid Films* **326** 205
[19] Kraus W A and Schatz G C 1983 *J. Chem. Phys.* **79** 6130
[20] Hövel H, Fritz S, Hilger A and Kreibig U 1993 *Phys. Rev.* B **48** 18178
[21] Gadenne M, Podolskiy V, Gadenne P, Sheng P and Shalaev V M 2001 *Europhys. Lett.* **53** 364
[22] Anno E and Tanimoto M 2000 *J. Appl. Phys.* **88** 3426
[23] Cattaruzza E, Battaglin G, Gonella F, Polloni R, Mattei G, Maurizio C, Mazzoldi P, Sada C, Montagna M, Tosello C and Ferrari M 2002 *Phil. Mag.* B **82** 735
[24] Mu R, Chen J, Gu Z Y, Ueda A, Tung Y-S, Henderson D O, White C W, Zhu J G, Budai J D and Zuhr R A 1997 *Mater. Res. Soc. Symp. Proc.* **438** 441
[25] Morimoto T, Sanada Y and Tomonaga H 2001 *Thin Solid Films* **392** 214
[26] Schroeder W, Wiggenhauser H, Schrittenlacher W and Kolb D M 1987 *J. Chem. Phys.* **86** 1147
[27] Kingery W D, Bowen H K and Uhlmann D R 1976 *Introduction to Ceramics* (New York: Wiley)
[28] Weaver J H 1975 *Phys. Rev.* B **11** 1416
[29] Ershov B G and Sukhov N L 2001 *Russ. J. Phys. Chem.* **75** 1303
[30] Gao T-R, Chen Z-Y, Peng Y and Li F-S 2002 *Chin. Phys.* **11** 1307
[31] Paul A and Tiwari A N 1973 *Phys. Chem. Glasses* **14** 69
[32] Löbl H P, Huppertz M and Mergel D 1996 *Surf. Coat. Technol.* **82** 90
[33] Mennig M, Oliverira P W and Schmidt H 1999 *Thin Solid Films* **351** 99
[34] Bae D-S, Han K-S and Adair J H 2002 *J. Am. Ceram. Soc.* **85** 1321
[35] Miyao T, Toyoizumi N, Okuda S, Imai Y, Tajima K and Naito S 1999 *Chem. Lett.* 1125
[36] Anders H 1967 *Thin Films in Optics* (London: The Focal Press)
[37] Born M and Wolf E 1975 *Principles of Optics* (New York: Pergamon)
[38] Pettit R B, Brinker C J and Ashley C S 1985 *Sol. Cells* **15** 267
[39] Gombert A, Rose K, Heinzel A, Horbelt W, Zanke C, Bläsi B and Wittwer V 1998 *Sol. Energy Mater. Sol. Cells* **54** 333